CrossMark

RESEARCH PAPER

One-step synthesis of monodisperse AuNPs@PANI composite nanospheres as recyclable catalysts for 4-nitrophenol reduction

Runming Li · Zhiyuan Li · Qiang Wu · Dongfeng Li ·
Jiahua Shi · Yuewen Chen · Shuling Yu · Tao Ding ·
Congzhen Qiao

Abstract Oxidative polymerization of aniline was carried out in ethanol using chloroauric acid (HAuCl₄) as the oxidant. Simultaneous reduction of HAuCl₄ and formation of gold nanoparticles (AuNPs) and polyaniline (PANI) composite nanospheres (AuNPs@PANI nanospheres) were achieved without using any templates or structure-directing agents. The composite nanospheres are uniformly distributed with an average diameter of about 400 nm, in which the ultrafine AuNPs with size of about 2–4 nm were evenly embedded in the PANI matrix which acted as the dispersing agent and stabilizer of AuNPs. In addition, the catalytic performance of these composite nanospheres towards the reduction of 4-nitrophenol in the presence of NaBH₄ was studied. Furthermore, the possible formation mechanism and catalytic mechanism of the self-assembled AuNPs@PANI nanospheres were also discussed.

Introduction

Gold nanoparticles (AuNPs) have attracted considerable attention in the fields of nanotechnology and material science owing to their unique catalytic, optical, biological, medical, magnetic and electronic properties which make them suitable for potential applications in catalysis (Yu et al. 2016; Chen et al. 2016; Wang et al. 2016), sensors (Rana et al. 2016; Schlicke et al. 2016; Maji et al. 2016), biomedicine (Liu et al. 2015; Dreaden et al. 2012; Joseph et al. 2014), fluorescence imaging (Zhang et al. 2015), surface-enhanced Raman scattering (Li et al. 2016; Xie et al. 2014; Xiang et al. 2016; Schürmann and Bald 2016), electronics and photonics (Luechinger et al. 2008). In particular, since Haruta's discovery of high catalytic activity of AuNPs for low-temperature oxidation of CO (Haruta et al. 1987), the exploration of gold nanocatalysts for a variety of catalytic reactions has been a hot research topic. However, free-standing AuNPs tend to aggregate, drop or dissolve during catalytic reactions so that their original catalytic activities will gradually reduce or disappear after several cycles of catalysis. To overcome these disadvantages, much effort has been paid to anchor

R. Li · Z. Li · Q. Wu · D. Li · J. Shi (✉) ·
Y. Chen · S. Yu · T. Ding · C. Qiao
Institute of Fine Chemical and Engineering, Engineering Laboratory for Flame Retardant and Functional Materials of Henan Province, College of Chemistry and Chemical Engineering, Henan University, Kaifeng 475004, China
e-mail: sjiahua@henu.edu.cn

AuNPs on or into various solid supports including polymers (Percebom et al. 2016; Quan et al. 2016; Zyuzin et al. 2016), metal oxides (Korotcenkov et al. 2016; Wang et al. 2014; Ishida et al. 2015; Padbury et al. 2015; Zhao et al. 2015), silica (Laveille et al. 2016), carbon materials (Carabineiroa et al. 2013; Lozano-Martín et al. 2015; Simenyuk et al. 2015; Nakashima et al. 2013) and biomaterials (Wei and Lu 2012; Lam et al. 2012).

Among these candidates for catalyst supports, polyaniline (PANI), as one of the most remarkable conducting polymers, has been recently recognized as a new class of supports for stabilizing AuNPs due to the facile and effective fabrication routes and potential applications in many areas. Up to now, various PANI/Au nanocomposite materials have been prepared. Yang and Kaner et al. have demonstrated the electrical bistability and memory effect of AuNPs-decorated PANI nanofibres by reduction of $HAuCl_4$ on PANI nanofibres as reducing agent (Tseng et al. 2005; Baker et al. 2011). Recently, AuNPs-decorated PANI nanofibres, nanotubes and nanospheres were achieved and the catalytic activity of these composites was studied (Qiao et al. 2015; Zhang et al. 2016; Dutt et al. 2015). Furthermore, through a chemical redox reaction between $HAuCl_4$ and 2-aminothiophenol, Guo et al. also synthesized poly(2-aminothiophenol) and AuNPs composites which can be used as efficient catalysts for Suzuki–Miyaura crosscoupling reaction and the reduction of 4-nitrophenol in the presence of sodium borohydride ($NaBH_4$) (Han et al. 2009, 2011). In addition, raspberry-like, sphere-like and rod-like PANI/Au nanocomposites were successfully obtained with the help of different surfactants (Xu et al. 2012; Huang et al. 2006, 2012).

Although a variety of PANI/Au nanocomposite materials were successfully synthesized, it was seldom reported that many AuNPs were embedded uniformly in PANI matrix (denoted as AuNPs@PANI nanocomposites) rather than attached on the surface of PANI. AuNPs deposited on the surface of PANI tend to drop and deactivate upon long-term exposure in the reaction solution. Therefore, the design and synthesis of encapsulating many fine AuNPs into PANI matrix to form AuNPs@PANI nanocomposites with good catalytic activity and high stability is still a great challenge. Herein, we report a facile, rapid and one-step synthesis of uniformly distributed and monodisperse AuNPs@PANI composite nanospheres via oxidative polymerization of aniline by using $HAuCl_4$ as oxidant in ethanol without the aid of any templates and additives. The ultrafine AuNPs were embedded evenly in the PANI matrix which acted as the dispersing agent and stabilizer of AuNPs. In addition, the catalytic performance of these composite nanospheres was evaluated towards the reduction of 4-nitrophenol in the presence of $NaBH_4$. Furthermore, the possible formation mechanism and catalytic mechanism of the self-assembled AuNPs@PANI nanospheres were also discussed.

Experimental details

Materials

Aniline monomer (500 mL, purchased from Sigma-Aldrich) was distilled under reduced pressure before use. The middle white distillate was collected between 85 and 110 °C. Chloroauric acid tetrahydrate ($HAuCl_4\cdot4H_2O$) was purchased from Sigma-Aldrich. All other reagents were purchased from Aladdin Reagent Co. Ltd. and used without further purification.

Preparation of AuNPs@PANI composite nanospheres

In a typical synthesis, 0.2 mmol aniline and 0.067 mmol $HAuCl_4\cdot4H_2O$ were dissolved in 20 mL of ethanol, respectively. Then, the two solutions were mixed rapidly. The reaction was carried out at room temperature without any disturbance for 24 h. The resulting precipitates were centrifuged at 10,000 rpm using a TG16-WS Centrifuge and washed with water and ethanol several times. Finally, the products were dried under vacuum (DZF-6020 vacuum oven) at 50 °C for 24 h. Some control experiments were also carried out by varying the molar ratio and concentration of oxidant and monomer.

Preparation of hollow PANI nanospheres with nanocavities

The as-prepared AuNPs@PANI composite nanospheres were dried under vacuum at 50 °C for 24 h. The dried products were then soaked in saturated I_2/KI solution with shaking on a HY-4 table concentrator for 12 h. Finally, the products were centrifuged and

washed successively with KI aqueous solution and distilled water several times. The final products were dried under vacuum at 50 °C for 24 h.

Catalytic reduction of 4-nitrophenol to 4-aminophenol by AuNPs@PANI composite nanospheres

Catalytic properties of the synthesized AuNPs@PANI nanospheres were investigated via the reduction of 4-nitrophenol (4-NP) to 4-aminophenol (4-AP) with NaBH$_4$ as reducing agent. Typically, 1.0 mL of 4-NP aqueous solution (0.25 mM) and 2.0 mL of freshly prepared NaBH$_4$ (10 mM) aqueous solution were mixed to form a homogeneous reaction solution in a quartz cuvette. Then, 0.15 mL of the as-prepared AuNPs@PANI composite nanosphere suspensions was added to the above mixture with gentle shaking. The progress of the conversion of 4-NP to 4-AP was quickly monitored via UV–Vis spectroscopy by recording the time-dependent adsorption spectra of the reaction mixture at ambient temperature. In the recycling study, after the reduction was completed in several minutes, the catalyst was separated by centrifugation, washed with water, and reused in the next reaction run.

Characterization and instrumentation

The scanning electron microscope (SEM) images of samples were taken with a JEOL JSM-6701F field emission SEM and transmission electron microscope (TEM) observations were performed on a JEOL JEM2011 at 200 kV equipped with selective area electron diffraction (SAED). The chemical and electronic structures of samples were studied using a Fourier transform infrared spectrometer (FTIR, AVA-TAR360) and UV–Visible spectrophotometer (UV–Vis, U-4100). X-ray diffraction (XRD) patterns were acquired by a Bruker AXS D5005 X-ray powder diffractometer with Cu Kα radiation. Thermogravimetric analysis (TGA) was carried out at a heating rate of 20 °C/min on an EXSTAR 6000 TGA in air.

Results and discussion

The oxidation polymerization of aniline was carried out using HAuCl$_4$ in ethanol as the oxidant by simultaneous reduction of HAuCl$_4$ to gold nanostructures at room temperature. At the theoretical HAuCl$_4$/aniline molar ratio of 1:3 and monomer concentration of 5.0 mM, SEM images shown in Fig. 1a clearly reveal that the obtained products are monodisperse and regular nanospheres. At a higher magnification as shown in Fig. 1b, these nanospheres are uniformly distributed with an average diameter of about 400 nm. The structure of the synthesized nanospheres was further observed by TEM, as shown in Fig. 1c, which proved that the spheres are solid with smooth surface. An electron diffraction (ED) pattern (Fig. 1c inset) of this area showed the characteristic ring corresponding to the amorphous PANI spheres and the diffraction spots due to nanoscale gold. Where is the gold? High-resolution TEM was used to further observe the edge part of a nanosphere, as shown in Fig. 1d, the highly dispersed black dots with size of about 2–4 nm are evenly embedded in the nanosphere, which is different from the AuNPs-decorated PANI nanocomposites by a two-step method where AuNPs are always deposited on outer surfaces of PANI matrix (Tseng et al. 2005; Baker et al. 2011; Han et al. 2010). These black dots with different crystalline structures should be ascribed to AuNPs that come from reduction of HAuCl$_4$. So the as-prepared nanospheres can be called AuNPs@PANI composite nanospheres. The XRD patterns of the resulting nanospheres are shown in the supporting information (Fig. S1). The broad peak centred at $2\theta = 29°$ is ascribed to PANI. There are four main peaks at 38, 44, 65 and 78° in the XRD patterns of the resulting products, which correspond to (111), (200), (220) and (311) Bragg reflections of nano-sized gold, respectively, further confirming the coexistence of gold and PANI nanospheres.

In order to explore the distribution of AuNPs in the composite spheres, the as-prepared AuNPs@PANI composite nanospheres were immersed in saturated I$_2$/KI solution to remove the AuNPs embedded in polymer matrix. The morphology and inner structure of the final powder after removal of AuNPs can be observed in the SEM and TEM images shown in Fig. S2. The hollow PANI spheres retain the spherical structures within continuous or continuous nanocavities, which prove the uniform distribution of AuNPs in the nanospheres. To further determine the gold content in the as-prepared AuNPs@PANI composites, PANI was removed by calcination in a TGA instrument. Figure S3 presents the mass loss curve of the
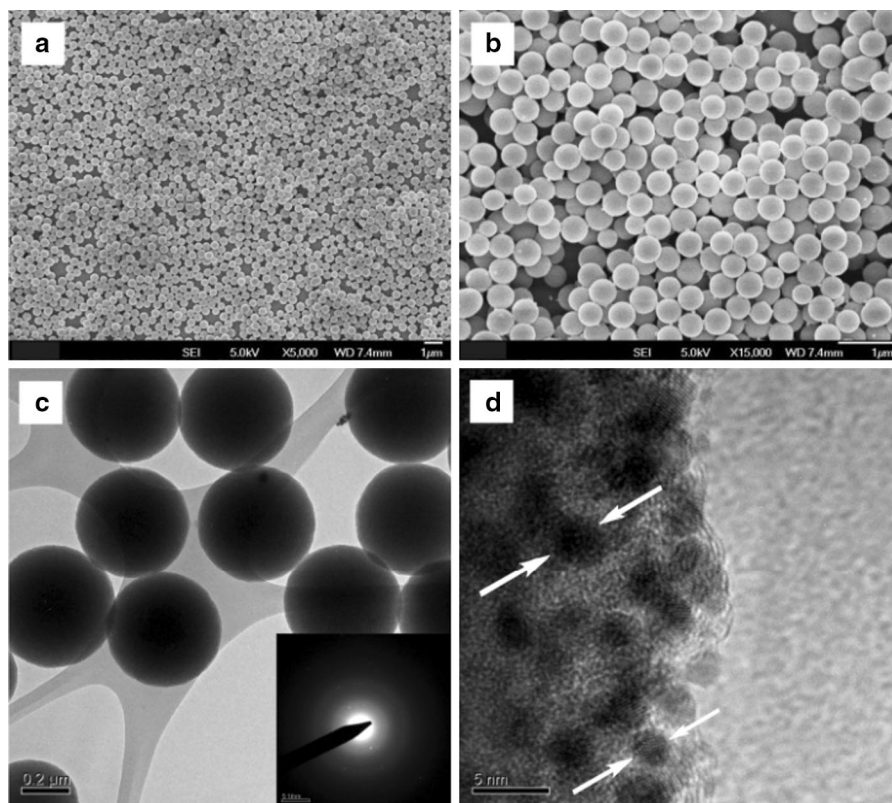
Fig. 1 SEM and TEM images of the as-prepared products. **a**, **b** SEM image of AuNPs@PANI nanospheres at a different magnification; **c** TEM image of complete AuNPs@PANI nanospheres; **d** TEM image of an edge part of AuNPs@PANI nanospheres

sample upon heating in air. There were mainly two weight-loss stages when the sample was heated from room temperature to 700 °C. The weight loss before ~ 560 °C should be attributed to the loss of PANI with different molecular weights. The residual sample mass fraction representing the gold content was about 33 %.

The chemical and electronic structures of the as-prepared AuNPs@PANI spheres and hollow PANI spheres were studied by UV–Vis and FTIR spectroscopies, respectively. As shown in Fig. 2a, AuNPs@PANI nanospheres had two obvious UV–Vis absorption peaks located at 320 and 530 nm, respectively. The absorption peak at 320 nm corresponded to $\pi–\pi^*$ electron transition of the benzenoid rings. The wide absorption peak at 530 nm was the synergetic effect between surface plasmon resonance of AuNPs and $n–\pi^*$ electron transition associated with a benzenoid-to-quinoid excitonic transition (Shi et al. 2013; Shiigi et al. 2006; Neoh et al. 1993). After the removal of AuNPs, the $\pi–\pi^*$ electron transition band of

benzenoid rings shifts from 320 to 285 nm and the $n–\pi^*$ absorbance between 480 and 560 nm appears without AuNPs synergy. The FTIR spectra of PANI nanospheres before and after dissolving AuNPs are presented in Fig. 2b for comparison. The characteristic PANI peaks located at 1596 and 1498 cm^{-1} correspond to the C=C stretching deformation of quinoid and benzenoid rings, respectively (Shi et al. 2013; Li et al. 2001; Stejskal et al. 2008). The peaks at 1384, 1308 and 1242 cm^{-1} belong to C–N stretching vibration (Kang et al. 1998). The peak at 825 cm^{-1} is assigned to the presence of para-disubstituted rings, while the two peaks at 696 and 755 cm^{-1} are attributed to the corresponding C–H out-of-plane bending vibrations of the monosubstituted benzene ring, indicating that the PANI nanospheres are aniline oligomers (Kang et al. 1998).

In order to explore the formation mechanism of AuNPs@PANI nanospheres, we investigated the effect of molar ratio and concentration of oxidant
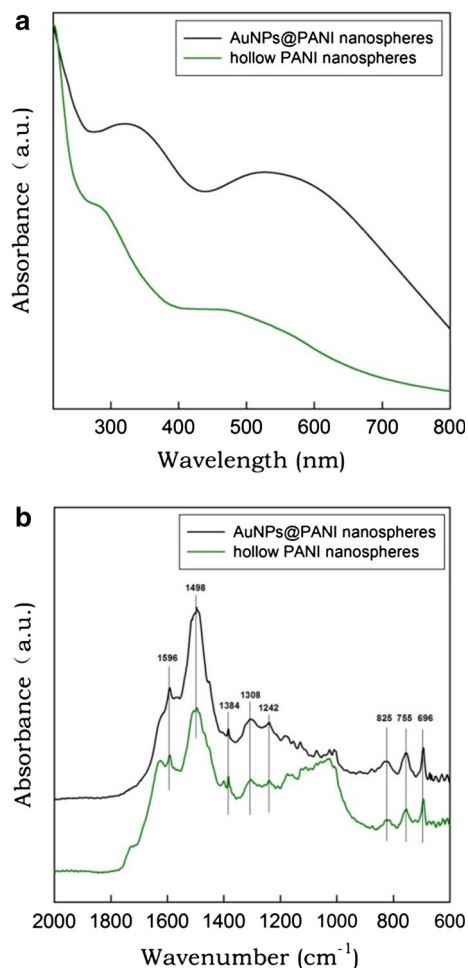
Fig. 2 FTIR (a) and UV–Vis absorption spectra (b) of AuNPs@PANI nanospheres and hollow PANI nanospheres

and monomer on the morphology and size of resulting PANI/Au nanocomposites. When the amount of aniline was kept at 5.0 mM and the molar ratio of $HAuCl_4$/aniline was adjusted from 1:3 to 1:2 and 1:5, it was found that the morphology and size of prepared products changed accordingly. At $HAuCl_4$/aniline ratio of 1:2, as shown in Fig. 3a, b, c, the spherical morphology of PANI/Au composite remained; nevertheless, the average size of spheres increased to microlevel. The high-resolution TEM image proved that fine AuNPs with 2–4 nm were also incorporated in PANI microspheres. When the molar ratio of $HAuCl_4$/aniline decreased to 1:5, nanoparticles with average diameter of ~200 nm were obtained (Fig. 3d, e). These nanoparticles should be Au@PANI core–shell nanoparticles which are AuNPs capped with a thin

layer of PANI with thicknesses of about 10 nm. This was confirmed by HR-TEM shown in Fig. 3f.

At the fixed $HAuCl_4$/aniline ratio of 1:3, Fig. 4 shows the effect of monomer concentration on the morphology and size of products. When aniline concentration was 3.0 and 50 mM, respectively, the spherical morphologies of the as-prepared samples were still yielded. With increasing the concentration of aniline from 3.0 to 5.0 and 50 mM, compared with Fig. 1, the average diameters of the spheres increased from around 200–400 nm and 1 μm accordingly. High-resolution TEM further proved that the spherical products were all AuNPs@PANI composites with fine AuNPs incorporated into PANI spheres (Fig. S4). At the given oxidant/aniline ratio of 1:3, lower concentration of monomer favours the AuNPs@PANI spheres with smaller size. At higher monomer concentration, however, a large amount of aniline will induce fast reaction and form larger spheres with various sizes.

Therefore, the proposed formation mechanism of AuNPs@PANI nanospheres is shown in Fig. 5. $HAuCl_4$ and aniline dissolved in ethanol to form a homogenous solution. Due to the weak oxidizability of $HAuCl_4$ in acidic ethanol solution, aniline oligomer and small-sized gold nuclei would be inclined to be generated during the oxidation–reduction reaction. The formed gold nuclei and aniline oligomer can be well dispersed in ethanol. In addition, due to the strong interaction between Au atom and aniline oligomer containing a lot of p–π conjugate amino groups, aniline oligomers could act as the dispersing agent and stabilizer to adsorb on gold nuclei and protect gold nuclei from aggregation (Han et al. 2012). When the molar ratio of $HAuCl_4$/aniline is greater than or equal to 1:3, an adequate amount of $HAuCl_4$ will induce relatively fast redox reaction to generate more gold nuclei and aniline oligomer. Further, because of the good solubility of aniline oligomers in ethanol and a strong interaction between the aniline oligomers (Shiigi et al. 2006), aniline oligomers protecting gold nuclei tend to aggregate together to form spherical AuNPs@PANI composite which possesses a minimum surface tension. However, at the fixed aniline concentration, the amount of $HAuCl_4$ decreased significantly when the molar ratio of $HAuCl_4$/aniline decreased from 1:3 to 1:5, which resulted in lower reaction rate to form less gold nuclei and aniline oligomer. Therefore, the resulting gold nuclei will
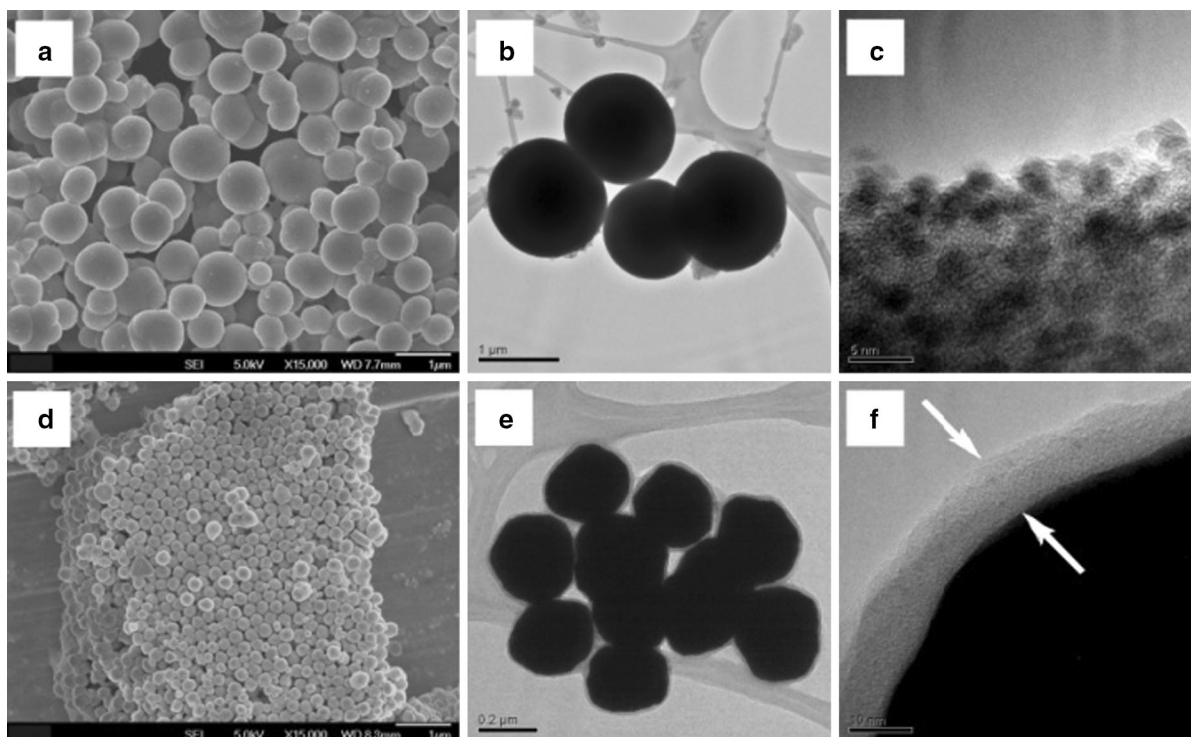
Fig. 3 SEM and TEM of PANI/Au powder synthesized at other molar ratios of HAuCl$_4$/aniline: (**a**, **b**, **c**) 1:2; (**d**, **e**, **f**) 1:5. Other reaction conditions: [aniline] = 5.0 mM, 25 °C, t = 24 h
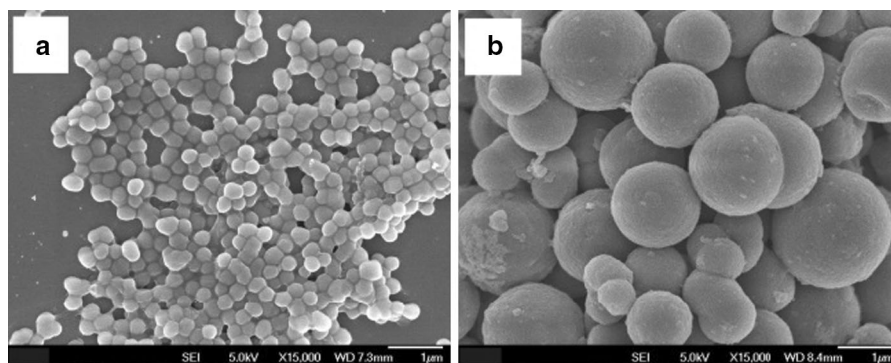
Fig. 4 SEM of AuNPs@PANI powder synthesized at different monomer concentrations: **a** 3.0 mM; **b** 50 mM. Other reaction conditions: the molar ratio of HAuCl$_4$/aniline is 1:3, 25 °C, t = 24 h

have enough time to recrystallize into large-sized Au@PANI core–shell nanoparticles by Ostwald ripening. In this reaction, ethanol played a vital role in preparing AuNPs@PANI nanospheres as it reduced the oxidizability of oxidant and dispersed the product promptly at different reaction stages.

Gold had long been considered an inert metal until Haruta et al. (1987) found that nano-sized gold deposited on ferric oxide or titanium dioxide showed high catalytic performance for carbon monoxide low-temperature oxidation. It is generally believed that AuNPs with size less than 10 nm have high catalytic performance (Haruta 1997). Until now, many catalytic applications of AuNPs have been reported, such as the oxidation of carbon monoxide (Haruta et al. 1987; Peng et al. 2008), ethanol (Feng et al. 2012;

Fig. 5 Schematic illustration of the formation of AuNPs@PANI composite nanospheres
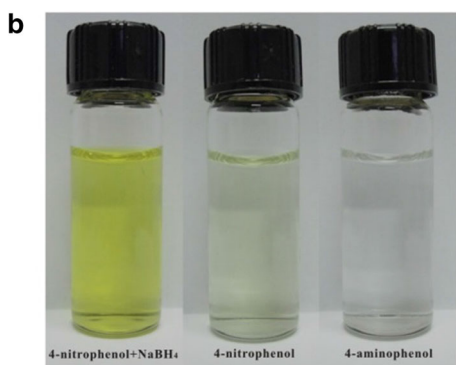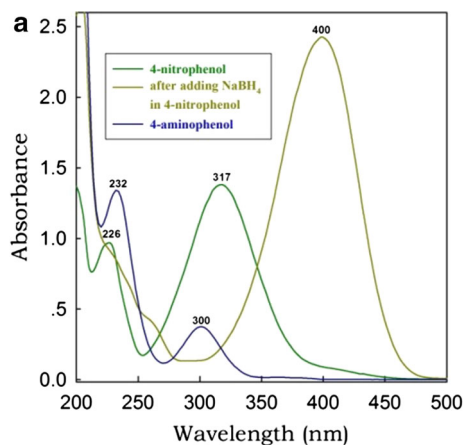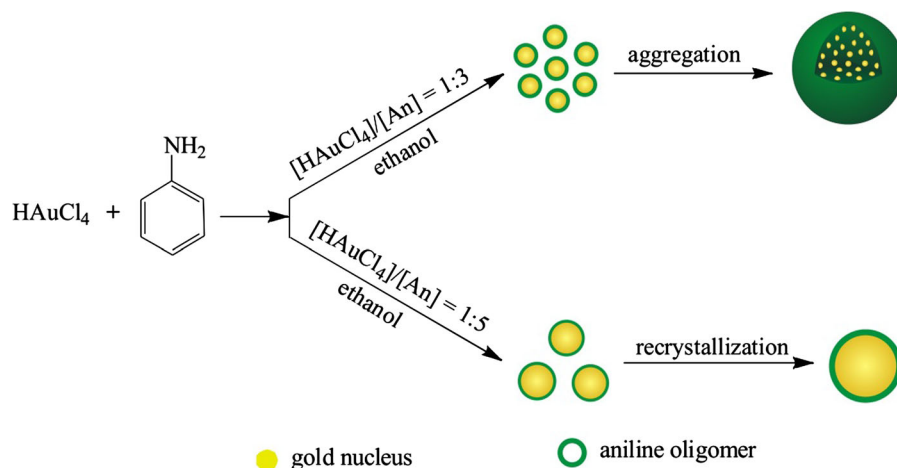
Fig. 6 UV–Vis absorption spectra (**a**) and images (**b**) of 4-nitrophenol, 4-nitrophenol added NaBH$_4$ and 4-aminophenol

Wu et al. 2012), etc. Here, the reduction of 4-NP to 4-AP with NaBH$_4$ as the reductant in aqueous solution was chosen as a model system to evaluate the catalytic performance of the as-prepared AuNPs@PANI composite nanospheres. UV–Vis absorption spectra and the colour change of the reaction solution were used to monitor the catalytic process of oxidation–reduction reaction. As shown in Fig. 6a, the initial aqueous 4-NP solution exhibited two absorption peaks at 226 and 317 nm. Upon the addition of freshly prepared NaBH$_4$ aqueous solution, the absorption peak at 226 nm disappeared and the absorption maximum at 317 nm shifted to 400 nm due to the formation of 4-nitrophenolate ion under the alkaline conditions, which resulted in a colour change of the solution from light yellow to yellow-green (Fig. 6b). In fact, the absorption intensity at 400 nm was almost unchanged even after 6 h, indicating that it was difficult for the reduction reaction to proceed without a catalyst. However, after the addition of a trace amount of AuNPs@PANI nanospheres, the absorption peak at 400 nm disappeared and a new absorption peak at 300 nm appeared, indicating the successful transformation of 4-NP to 4-AP (Fig. 6a). This reduction reaction is also visualized by the decolorization of the characteristic yellow-green colour of the solution (Fig. 6b). The Au@PANI core–shell nanoparticles and hollow PANI nanospheres were also tested as a control, and they showed no catalytic performance.

The UV–Vis absorption spectra were used to monitor the detailed change of absorption intensity at 400 nm during the catalytic reaction of 4-NP. Figure 7 displays a typical time-dependent evolution

Tsunoyama et al. 2009), glucose (Tokonami et al. 2010) and the reduction of rhodamine B (RhB) dye (Zhang et al. 2012), 4-nitrophenol (Han et al. 2010; Jiang et al. 2011; Liu et al. 2011; Shin and Huh 2012;
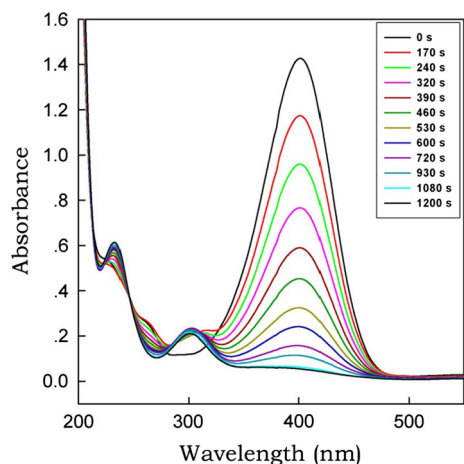
Fig. 7 Successive UV–Vis absorption spectra of the catalytic reduction of 4-nitrophenol to 4-aminophenol by NaBH$_4$ in the presence of AuNPs@PANI nanospheres as catalysts for the first time

of UV–Vis absorption spectra of 4-NP to 4-AP by NaBH$_4$ in the presence of AuNPs@PANI nanospheres as catalysts for the first time. The absorption peak at 400 nm gradually decreased in intensity and disappeared completely after 20 min along with the increase of a new absorption peak at 300 nm attributed to 4-AP.

Because of the much higher concentration of the NaBH$_4$ than 4-NP in the reaction system, this reaction can be considered as a pseudo-first-order reaction with regard to 4-NP. Therefore, the reaction kinetics can be described as $\ln(C_t/C_0) = -kt$, where k is the first-order rate constant (s^{-1}), t is the reaction time, C_t and C_0 are the concentrations of 4-NP at time t and 0, respectively. Figure 8a shows

$\ln C_t/C_0$ versus the reaction time t in the reduction of 4-NP by AuNPs@PANI nanospheres used for the different cycles. It was found that there was an initial delay before the onset of rapid catalytic reaction. This delay can be caused by the diffusion of the reactants to the surface of AuNPs by way of PANI coating. Discarding the initial delay, the plot follows first-order reaction kinetics very well. The rate constant k can be obtained from the slope of a linear plot of $\ln(C_t/C_0)$ versus reduction time. The linear relation also confirmed the pseudo-first-order kinetics. The rate constant k for the first time obtained directly from the slope of the straight line was found to be 3.09×10^{-3} s^{-1} for AuNPs@PANI nanosphere catalyst. It should be noted that a slight decrease in the rate constant was observed when the catalyst was reused for six cycles (Fig. 8a). The slow and gradual decline in catalytic performance during the recycling process was probably caused by the partial loss of AuNPs@PANI nanospheres during the centrifugal separation process.

Stability and recyclability are of great importance for practical application of catalyst. In our catalytic system, the solid catalyst was easily recovered from the reaction mixture by centrifugation. Then the AuNPs@PANI nanosphere catalyst was reused under the same reaction conditions for subsequent cycles to evaluate the recyclability. As shown in Fig. 8b, the AuNPs@PANI nanosphere catalyst can be successfully recycled and reused for six successive cycles of reaction with a conversion efficiency of around 100 % within 30 min, indicating the excellent stabilization ability and recoverable catalytic activity of the AuNPs@PANI nanospheres.

Fig. 8 **a** Plot of $\ln(C_t/C_0)$ versus time for the reduction of 4-nitrophenol in six successive cycles of reduction; **b** conversion of 4-nitrophenol to 4-aminophenol within 30 min in six successive cycles of reduction by AuNPs@PANI nanospheres as catalysts

The possible mechanism of catalytic reduction of 4-NP by AuNPs@PANI nanospheres was proposed as follow. The activity of the Au atoms on the surface of AuNPs is very strong because the surface Au atoms are unsaturated and easy to coordinate with the S, N, O and B atoms containing lone pair electrons. The smaller the AuNPs size is, the higher the catalytic activity is. Embedding within PANI matrix evenly, AuNPs with the size of about 2–4 nm can coordinate well with B and N atoms and act as electron-transfer channel in this catalytic reaction (Lin and Doong 2011; Huang et al. 2009). Although AuNPs were coated with a thin layer of PANI, BH_4^- and 4-NP could diffuse from aqueous solution to the surface of AuNPs via PANI and then the electrons of BH_4^- could be transferred to 4-NP by mediating of AuNPs in AuNPs@PANI nanospheres. So it is reasonable to explain that there is an induction period before the beginning of the catalytic reaction. In this regard, the resulting reduction product 4-AP is easy to adsorb onto the surface of AuNPs in the AuNPs@PANI nanospheres, which can hinder the reactant 4-NP from reaching the AuNPs surface, thus causing a longer reduction period in catalytic activity after the first use of catalyst.

Normally, AuNPs lose their catalytic activities quickly because of the agglomeration between AuNPs (Choudhary and Goodman 2002). However, for the as-prepared AuNPs@PANI nanospheres, we do not need to worry about the agglomeration as AuNPs are embedded evenly in the PANI matrix which can act as the dispersing agent and stabilizer of AuNPs. In general, the AuNPs@PANI nanospheres prepared by one-step method can be used as catalyst with good catalytic activity and high stability.

Conclusion

In summary, monodisperse AuNPs@PANI composite nanospheres were successfully achieved in ethanol by a simple one-step synthesis method. The AuNPs of size 2–4 nm are evenly encapsulated in monodisperse PANI nanospheres. The formation of AuNPs@PANI nanospheres is deeply dependent on the reaction solvent ethanol which reduced the oxidizability of oxidant $HAuCl_4$ and dispersed the product promptly at different reaction stages. In addition, the as-prepared AuNPs@PANI nanospheres exhibited a good catalytic activity and high reusability towards the reduction of

4-NP to 4-AP in the presence of $NaBH_4$ because the resultant ultrafine AuNPs do not agglomerate in the polymer matrix. We believe that our results would enrich the preparation method of PANI/Au nanocomposites and contribute to the potential applications of PANI/Au nanocomposites in catalytic, electrical, biological and optical fields.

References

Baker CO, Shedd B, Tseng RJ, Martinez-Morales AA, Ozkan CS, Ozkan M, Yang Y, Kaner RB (2011) Size control of gold nanoparticles grown on polyaniline nanofibers for bistable memory devices. ACS Nano 5:3469–3474

Carabineiroa SAC, Martinsb LMDRS, Avalos-Borja M, Buijnsters JG, Pombeiro AJL, Figueiredo JL (2013) Gold nanoparticles supported on carbon materials for cyclohexane oxidation with hydrogen peroxide. Appl Catal A 467:279–290

Choudhary T, Goodman D (2002) Oxidation catalysis by supported gold nano-clusters. Top Catal 21:25–34

Dong C, Li J, Cui P, Liu H, Yang J (2016) Gold-catalyzed formation of core–shell gold–palladium nanoparticles with palladium shells up to three atomic layers. J Mater Chem A 4:3813–3821

Dreaden EC, Alkilany AM, Huang X, Murphy C, El-Sayed M (2012) The golden age: gold nanoparticles for biomedicine. Chem Soc Rev 41:2740–2779

Dutt S, Siril PF, Sharma V, Periasamy S (2015) Goldcore–polyanilineshell composite nanowires as a substrate for surface enhanced Raman scattering and catalyst for dye reduction. New J Chem 39:902–908

Feng JJ, Li AQ, Lei Z, Wang AJ (2012) Low-potential synthesis of "clean" Au nanodendrites and their high performance toward ethanol oxidation. ACS Appl Mater Interfaces 4:2570–2576

Han J, Liu Y, Guo R (2009) Facile synthesis of highly stable gold nanoparticles and their unexpected excellent catalytic activity for Suzuki-Miyaura cross-coupling reaction in water. J Am Chem Soc 131:2060–2061

Han J, Li L, Guo R (2010) Novel approach to controllable synthesis of gold nanoparticles supported on polyaniline nanofibers. Macromolecules 43:10636–10644

Han J, Dai J, Li L, Fang P, Guo R (2011) Highly uniform self-assembled conducting polymer/gold fibrous nanocomposites: additive-free controllable synthesis and application as efficient recyclable catalysts. Langmuir 27:2181–2187

Han J, Fang P, Dai J, Guo R (2012) One-pot surfactantless route to polyaniline hollow nanospheres with incontinuous multicavities and application for the removal of lead ions from water. Langmuir 28:6468–6475

Haruta M (1997) Size- and support-dependency in the catalysis of gold. Catal Today 36:153–166

Haruta M, Kobayashi T, Sano H, Yamada N (1987) Novel gold catalysts for the oxidation of carbon monoxide at a temperature far below 0 °C. Chem Lett 16:405–408

Huang K, Zhang Y, Long Y, Yuan J, Han D, Wang Z, Niu L, Chen Z (2006) Preparation of highly conductive, self-assembled gold/polyaniline nanocables and polyaniline nanotubes. Chem A 12:5314–5319

Huang J, Vongehr S, Tang S, Lu H, Shen J, Meng X (2009) Ag dendrite-based Au/Ag bimetallic nanostructures with strongly enhanced catalytic activity. Langmuir 25:11890–11896

Huang YF, Park YI, Kuo C, Xu P, Williams DJ, Wang J, Lin CW, Wang HL (2012) Low-temperature synthesis of Au/polyaniline nanocomposites: toward controlled size, morphology, and size dispersity. J Phys Chem C 116:11272–11277

Ishida T, Aikawa S, Mise Y, Akebi R, Hamasaki A, Honma T, Ohashi H, Tsuji T, Yamamoto Y, Miyasaka M, Yokoyama T, Tokunaga M (2015) Direct C–H arene homocoupling over gold nanoparticles supported on metal oxides. ChemSusChem 8:695–701

Jiang HL, Akita T, Ishida T, Haruta M, Xu Q (2011) Synergistic catalysis of Au@Ag core-shell nanoparticles stabilized on metal-organic framework. J Am Chem Soc 133:1304–1306

Joseph D, Tyagi N, Geckeler C, Geckeler KE (2014) Protein-coated pH-responsive gold nanoparticles: microwave-assisted synthesis and surface charge-dependent anticancer activity. Beilstein J Nanotechnol 5:1452–1462

Kang E, Neoh K, Tan K (1998) Polyaniline: a polymer with many interesting intrinsic redox states. Prog Polym Sci 23:277–324

Korotcenkov G, Brinzari V, Cho B (2016) Conductometric gas sensors based on metal oxides modified with gold nanoparticles: a review. Microchim Acta 183:1033–1054

Lam E, Hrapovic S, Majid E, Chong JH, Luong JH (2012) Catalysis using gold nanoparticles decorated on nanocrystalline cellulose. Nanoscale 4:997–1002

Laveille P, Guillois K, Tuel A, Petit C, Basset JM, Caps V (2016) Durable PROX catalyst based on gold nanoparticles and hydrophobic silica. Chem Commun 52:3179–3182

Li XG, Duan W, Huang MR, Yang YL (2001) Preparation and characterization of soluble terpolymers from m-phenylenediamine, o-anisidine, and 2,3-xylidine. J Polym Sci Part A 39:3989–4000

Li Y, Shi W, Chopra N (2016) Functionalization of multilayer carbon shell-encapsulated gold nanoparticles for surface-enhanced Raman scattering sensing and DNA immobilization. Carbon 100:165–177

Lin FH, Doong R-A (2011) Bifunctional Au-Fe$_3$O$_4$ heterostructures for magnetically recyclable catalysis of nitrophenol reduction. J Phys Chem C 115:6591–6598

Liu R, Mahurin SM, Li C, Unocic RR, Idrobo JC, Gao H, Pennycook SJ, Dai S (2011) Dopamine as a carbon source: the controlled synthesis of hollow carbon spheres and yolk-structured carbon nanocomposites. Angew Chem Int Ed 50:6799–6802

Liu G, Li Q, Ni W, Zhang N, Zheng X, Wang Y, Shao D, Tai G (2015) Cytotoxicity of various types of gold-mesoporous silica nanoparticles in human breast cancer cells. Int J Nanomed 10:6075–6087

Lozano-Martín MC, Castillejos E, Bachiller-Baeza B, Rodríguez-Ramos I, Guerrero-Ruiz A (2015) Selective 1,3-butadiene hydrogenation by gold nanoparticles on novelnanocarbon materials. Catal Today 249:117–126

Luechinger NA, Athanassiou EK, Stark WJ (2008) Graphene-stabilized copper nanoparticles as an air-stable substitute for silver and gold in low-cost ink-jet printable electronics. Nanotechnology 19:445201

Maji S, Cesur B, Zhang Z, De Geest BG, Hoogenboom R (2016) Poly(N-isopropylacrylamide) coated gold nanoparticles as colourimetric temperature and salt sensors. Polym Chem 7:1705–1710

Nakashima D, Marken F, Oyama M (2013) Indirect modification of glassy carbon with gold nanoparticles using non-conducting support materials. Electroanalysis 25:975–982

Neoh K, Kang E, Tan K (1993) Protonation and deprotonation behaviour of amine units in polyaniline. Polymer 34:1630–1636

Padbury RP, Halbur JC, Krommenhoek PJ, Tracy JB, Jur JS (2015) Thermal stability of gold nanoparticles embedded within metal oxide frameworks fabricated by hybrid modifications onto sacrificial textile templates. Langmuir 31:1135–1141

Peng S, Lee Y, Wang C, Yin H, Dai S, Sun S (2008) A facile synthesis of monodisperse Au nanoparticles and their catalysis of CO oxidation. Nano Res 1:229–234

Percebom AM, Giner-Casares JJ, Claes N, Bals S, Loh W, Luis M, Liz-Marzán LM (2016) Janus gold nanoparticles obtained via spontaneous binary polymer shell segregation. Chem Commun 52:4278–4281

Qiao X, Liu X, Li X, Xing S (2015) Anchoring gold nanoparticles inside polyaniline shells with magnetic cores for the enhancement of catalytic stability. New J Chem 39:8588–8593

Quan X, Peng CW, Dong J, Zhou J (2016) Structural properties of polymer-brush-grafted gold nanoparticles at the oil–water interface: insights from coarse-grained simulations. Soft Matter 12:3352–3359

Rana D, Jamwal D, Katoch A, Thakur P, Kalia S (2016) Eicosyl ammoniums elicited thermal reduction alleyway towards gold nanoparticles and their chemo-sensor aptitude. Analyst 141:2208–2217

Schlicke H, Rebber M, Kunze S, Vossmeyer T (2016) Resistive pressure sensors based on freestanding membranes of gold nanoparticles. Nanoscale 8:183–186

Schürmann R, Bald I (2016) Decomposition of DNA nucleobases by laser irradiation of gold nanoparticles monitored by surface-enhanced Raman scattering. J Phys Chem C 120:3001–3009

Shi J, Wu Q, Li R, Zhu Y, Qin Y, Qiao C (2013) The pH-controlled morphology transition of polyaniline from nanofibers to nanospheres. Nanotechnology 24:175602

Shiigi H, Yamamoto Y, Yoshi N, Nakao H, Nagaoka T (2006) One-step preparation of positively-charged gold nanoraspberry. Chem Commun 41:4288–4290

Shin HS, Huh S (2012) Au/Au@polythiophene core/shell nanospheres for heterogeneous catalysis of nitroarenes. ACS Appl Mater Interfaces 4:6324–6331

Simenyuk GY, Zakharov YA, Pavelko NV, Dodonov VG, Pugachev VM, Puzynin AV, Manina TS, Barnakov CN, Ismagilov ZR (2015) Highly porous carbon materials filled with gold and manganese oxidenanoparticles for electrochemical use. Catal Today 249:220–227

Stejskal J, Sapurina I, Trchová M, Konyushenko EN (2008) Oxidation of aniline: polyaniline granules, nanotubes, and oligoaniline microspheres. Macromolecules 41:3530–3536

Tokonami S, Morita N, Takasaki K, Toshima N (2010) Novel synthesis, structure, and oxidation catalysis of Ag/Au bimetallic nanoparticles. J Phys Chem C 114:10336–10341

Tseng RJ, Huang J, Ouyang J, Kaner RB, Yang Y (2005) Polyaniline nanofiber/gold nanoparticle nonvolatile memory. Nano Lett 5:1077–1080

Tsunoyama H, Ichikuni N, Sakurai H, Tsukuda T (2009) Effect of electronic structures of Au clusters stabilized by poly (N-vinyl-2-pyrrolidone) on aerobic oxidation catalysis. J Am Chem Soc 131:7086–7093

Wang Y, Van de Vyver S, Sharma KK, Román-Leshkov Y (2014) Insights into the stability of gold nanoparticles supported on metal oxides for the base-free oxidation of glucose to gluconic acid. Green Chem 16:719–726

Wang S, Xin X, Zhang H, Shen J, Zheng Y, Song Z, Yang Y (2016) Stable monodisperse colloidal spherical gold nanoparticles formed by an imidazolium gemini surfactant-based water-in-oil microemulsion with excellent catalytic performance. RSC Adv 6:28156–28164

Wei H, Lu Y (2012) Catalysis of gold nanoparticles within lysozyme single crystals. Chem Asian J 7:680–683

Wu S, Dzubiella J, Kaiser J, Drechsler M, Guo X, Ballauff M, Lu Y (2012) Thermosensitive Au-PNIPA yolk-shell nanoparticles with tunable selectivity for catalysis. Angew Chem Int Ed 51:2229–2233

Xiang Q, Zhu X, Chen Y, Duan H (2016) Surface enhanced Raman scattering of gold nanoparticles supported on copper foil with graphene as a nanometer gap. Nanotechnology 27:075201

Xie HN, Lin Y, Mazo M, Chiappini C, Sánchez-Iglesias A, Liz-Marzán LM, Stevens MM (2014) Identification of intracellular gold nanoparticles using surface-enhanced Raman scattering. Nanoscale 6:12403–12407

Xu X, Liu X, Yu Q, Wang W, Xing S (2012) Architecture-adapted raspberry-like gold@polyaniline particles: facile synthesis and catalytic activity. Colloid Polym Sci 290:1759–1764

Yu J, Xu D, Guan HN, Wang C, Huang LK, Chi DF (2016) Facile one-step green synthesis of gold nanoparticles using *Citrus maxima* aqueous extracts and its catalytic activity. Mater Lett 166:110–112

Zhang B, Zhao B, Huang S, Zhang R, Xu P, Wang HL (2012) One-pot interfacial synthesis of Au nanoparticles and Au–polyaniline nanocomposites for catalytic applications. CrystEngComm 14:1542–1544

Zhang J, Li C, Zhang X, Huo S, Jin S, An FF, Wang X, Xue X, Okeke CI, Duan G, Guo F, Zhang X, Hao J, Wang PC, Zhang J, Liang XJ (2015) In vivo tumor-targeted dual-modal fluorescence/CT imaging using a nanoprobe co-loaded with an aggregation-induced emission dye and gold nanoparticles. Biomaterials 42:103–111

Zhang Z, Jiang Y, Chi M, Yang Z, Nie G, Xiaofeng L, Wang C (2016) Fabrication of Au nanoparticles supported on CoFe2O4 nanotubes by polyaniline assisted self-assembly strategy and their magnetically recoverable catalytic properties. Appl Surf Sci 363:578–585

Zhao G, Xin-Ping W, Chai R, Zhang Q, Gong X, Huang J, Yong L (2015) Tailoring nano-catalysts: turning gold nanoparticles on bulk metal oxides to inverse nano-metal oxides on large gold particles. Chem Commun 51:5975–5978

Zyuzin MV, Honold T, Carregal-Romero S, Kantner K, Karg M, Parak WJ (2016) Influence of temperature on the colloidal stability of polymer-coated gold nanoparticles in cell culture media. Small 12:1723–1731